

We are IntechOpen, the world's leading publisher of Open Access books Built by scientists, for scientists

6,900

Open access books available

186,000

International authors and editors

200M

Downloads

Our authors are among the

154

Countries delivered to

TOP 1%

most cited scientists

12.2%

Contributors from top 500 universities



WEB OF SCIENCE™

Selection of our books indexed in the Book Citation Index
in Web of Science™ Core Collection (BKCI)

Interested in publishing with us?
Contact book.department@intechopen.com

Numbers displayed above are based on latest data collected.
For more information visit www.intechopen.com



Waterborne Acrylic/CeO₂ Nanocomposites for UV Blocking Clear Coats

Miren Aguirre, María Paulis and Jose R. Leiza

Additional information is available at the end of the chapter

<http://dx.doi.org/10.5772/intechopen.81332>

Abstract

The encapsulation of inorganic nanoparticles into polymer particles opens the door to countless applications taking advantage of the properties of both phases. In this chapter the UV absorbing capacity of CeO₂ nanoparticles and the film forming capacity of acrylic polymers are combined. A synthetic route to produce waterborne acrylic/CeO₂ hybrid nanocomposites for UV absorbing coatings applications is presented. This strategy leads to encapsulated morphology of the CeO₂ nanoparticles into the polymer particles and therefore to the lack of agglomeration during film formation. A mathematical model developed for inorganic/organic hybrid systems is able to explain the morphology evolution from the initial monomer droplet to the polymer particles. The films cast from these latexes are transparent and show excellent UV absorption that increases with the amount of cerium oxide nanoparticles in the hybrid latex. Finally, the photoactivity behavior that the CeO₂ nanoparticles may have on the polymeric matrix is studied, discarding additional effects on the acrylic polymer matrix.

Keywords: waterborne polymer dispersions, CeO₂ nanoparticles, hybrid nanocomposites, encapsulation, UV absorption

1. Introduction

The incorporation of metal oxide nanoparticles into polymer matrices opens the way to the production of novel nanocomposite materials due to the synergetic effect of each phase in the final properties, as well as the possibility to use them in many different applications. In this direction, in the last decade, many authors have studied the benefits in properties that could be obtained when combining CeO₂ nanoparticles with polymers. For instance, catalytic [1–3], thermal [4], mechanical [5, 6], optical [7–9], anticorrosion [10–12], and barrier properties [13]

of polymers have been considerably improved with the incorporation of CeO₂ nanoparticles. Moreover, CeO₂ nanocomposites can find application in many different fields such as chemi-sensors and photocatalyst for environmental applications [14–16], temperature and humidity sensors [17] or extractants for yttrium ions [18].

Taking advantage of the excellent UV absorption capacity of the CeO₂ nanoparticles, it is really interesting to incorporate these nanoparticles into polymer matrices in the field of outdoor clear coatings. Waterborne acrylic polymers, synthesized mainly by emulsion polymerization process, are widely used as protective coatings for different surfaces due to their low toxicity and good quality film forming properties [19]. However, the main drawback of these coatings is the photodegradation they suffer under UV light. Traditionally, organic UV absorbers and hindered amine light stabilizers (HALS) were used, but due to the increasing environmental pressure to reduce the volatile organic compounds (VOC) content in coatings, the use of metal oxides such as TiO₂ [20, 21], ZnO [22, 23] and CeO₂ [24, 25] have been considered as an attractive alternative. All of them absorb radiation around 400 nm [26] and possess a band gap energy of around 3 eV [27], which makes them good candidates for UV absorption purposes. There are some works in which TiO₂ [28–31] and ZnO [32–35] nanoparticles have been incorporated into polymer matrices to improve the UV absorbance capacity of the coating. Nevertheless, the photocatalytic activity of CeO₂ nanoparticles is lower than that of TiO₂ and ZnO [36], which might prevent a faster degradation of the acrylic coatings due to the presence of the metal oxide, making CeO₂ nanoparticles ideal candidates for their incorporation into waterborne acrylic coatings.

In waterborne hybrid coatings, the final morphology of the hybrid system is governed by the different nature of the inorganic nanoparticles and polymer. Therefore, the control of the morphology of the hybrid system is challenging. The compatibility between both phases (thermodynamics) as well as the polymerization process (kinetics) will define the final morphology of the nanocomposite and thus, the final application [37]. In the literature a variety of CeO₂ nanoparticles (hydrophilic or hydrophobically modified) have been incorporated following different polymerization processes.

For instance, Fischer [2] and Mari [3] synthesized CeO₂/polystyrene (PS) and CeO₂/polymethylmethacrylate (PMMA) hybrids with raspberry like morphology, following the same procedure. They synthesized PS and PMMA latexes incorporating active groups (acrylic, methacrylic or phosphate groups) on the surface of either the PS or PMMA polymer particles, synthesized previously by miniemulsion polymerization. These active groups served as nucleating agents for the crystallization of the CeO₂. As the CeO₂ nanoparticles were generated in the surface of the polymer particles, this morphology was very favorable to take advantage of the catalytic behavior of the CeO₂, giving for instance very efficient catalyst for the hydration reaction of 2-cyanopyridine to 2-picolinamide.

Another possibility to obtain pickering morphology is to use the inorganic nanoparticles to stabilize the polymer particles. CeO₂ nanoparticles were used as pickering stabilizers in the miniemulsion polymerization of acrylates by Zgheib et al. [38]. It was found that at least 35 wt% of CeO₂ nanoparticles were necessary to obtain stable hybrid latexes at intermediate solids content (25 wt%). Therefore, the large amount of nanoparticles used and the solids content obtained, limited their application as coating. However, using other inorganic nanoparticles,

such as SiO₂ or TiO₂, it has been possible to obtain high solids content latexes [39]. The ability of these hybrid nanocomposites with Pickering morphology as protective coatings [40, 41] has been successfully proved.

Hawkett was the first one adsorbing amphiphilic macro-RAFT agents on the surface of inorganic nanoparticles and starting the polymerization from the macro-RAFT agents to obtain encapsulation of the inorganic nanoparticles [42, 43]. Garnier [44, 45], Warrant [46] and Zgheib [47] followed this method to encapsulate CeO₂ nanoparticles. The hybrid acrylic/ CeO₂ latexes were obtained by semibatch emulsion polymerization starting the polymerization from the macro-RAFT agent modified CeO₂ nanoparticles. In general, good distribution of the CeO₂ nanoparticles in the polymer particles was obtained and the CeO₂ nanoparticles were located close to particle-aqueous phase interface and even encapsulated in some examples.

In this Chapter, a polymerization approach to produce waterborne hybrid (polymer/CeO₂) dispersions with encapsulated CeO₂ nanoparticles will be presented. The prediction of the evolution of the morphology during the polymerization will be illustrated by means of a mathematical model and finally the UV absorbing properties of the clear coatings produced from these hybrid latexes and the potential photochemical degradation of the coatings will be discussed.

2. Synthesis of acrylic/CeO₂ hybrid nanocomposites by seeded semibatch (mini)emulsion polymerization

In the production of waterborne binders (for coatings), emulsion polymerization is the most popular process. However, when it comes into hybrid waterborne binders, miniemulsion polymerization emerged as an alternative process, to overcome the limitations of emulsion polymerization when the inorganic material must be incorporated into the polymer particles [48–50]. Moreover, equilibrium morphology simulations have demonstrated that if the nanoparticles present good wettability in the monomer phase, they can be encapsulated in monomer nanodroplets and hence hybrid latexes with encapsulated morphology can be produced [51].

The approach presented here to produce waterborne acrylic/CeO₂ nanocomposite dispersions uses a two-step seeded semibatch (mini)emulsion polymerization process. The approach is well suited to produce hybrid latexes with CeO₂ contents spanning between 0.5 and 5 wt% based on the polymer [52, 53]. In the first step, hybrid seed particles are synthesized by batch miniemulsion polymerization. In the second step the solids content and the final concentration of the CeO₂ nanoparticles can be tuned by controlling the composition of the feed of the semibatch process. Two feeding strategies can be used:

- (i) Neat monomer preemulsion feeding. A preemulsion is fed containing monomers, emulsifier and water, to grow the already formed seed hybrid particles. In this case, all the CeO₂ nanoparticles present in the final hybrid are only added in the seed prepared in the first step. Hybrid latexes with 40–50% solids content were synthesized [53, 54] with CeO₂ contents up to 1 wt% in the final hybrid composite.

- (ii) Hybrid monomer/CeO₂ miniemulsion feeding. The same formulation of the miniemulsion used to synthesize the seed is used as feed allowing higher concentration of CeO₂ in the final latex. Hybrid latexes with CeO₂ contents up to 5 wt% were obtained at 40% of solids content [55].

Figure 1 presents the transmission electron microscopy (TEM) images of relevant latexes with low (1 wt%) and high (5 wt%) content of CeO₂ nanoparticles produced using the two feeding strategies discussed above, respectively. As it can be seen, the polymer particle size

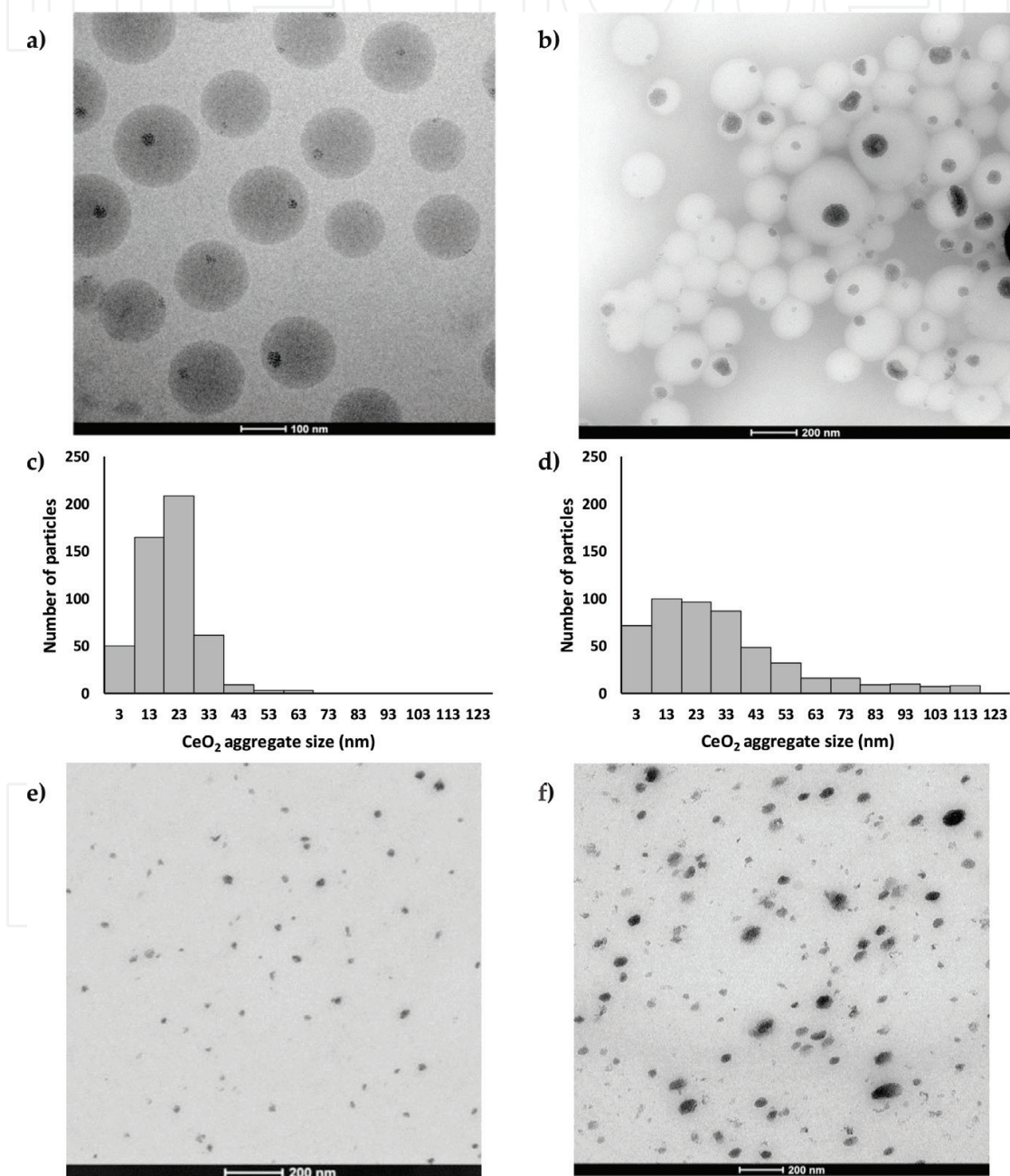


Figure 1. (a) Cryo-TEM image and (b) TEM image of the latexes, (c) and (d) CeO₂ aggregate size distributions in the hybrid latex and (e) and (f) TEM of the hybrid films for the sample containing 1% CeO₂ and 40% SC produced by neat monomer preemulsion feeding strategy (a,c,e) and for the sample containing 5% CeO₂ and 40% SC synthesized using the hybrid miniemulsion feeding (b,d,f).

distribution (PSD) obtained by both feeding strategies is different. Even if the PSD obtained for the hybrid seed is the same for both cases, with particles around 100 nm, the final PSD differs depending on the feeding strategy. When neat monomer preemulsion is fed (**Figure 1a**) the final PSD is narrow, suggesting lack of secondary nucleation during the semibatch process. Nevertheless, the PSD obtained when feeding the miniemulsion (second strategy) is broader, as particles between 25 and 600 nm can be found (**Figure 1b**). This is related to the miniemulsion stability and to the monomer droplet nucleation efficiency in the reactor. According to Rodriguez et al., the nucleation efficiency in a seeded semibatch miniemulsion polymerization is related to the stability of the miniemulsion fed (the higher the stability, the higher the nucleation of the entering droplets), and also to the ratio of the number of entering droplets with respect to the number of particles in the seed (the higher this ratio, the higher the number of fed droplets nucleate because their efficiency for capturing radical is higher) [56]. In **Figure 1b**, very small polymer particles can be seen containing nanoceria, which is an indication that hybrid monomer droplets serve as monomer reservoirs when they enter into the reactor, but they do not lose their identity and finally they end up nucleating [55, 57].

In any case, the CeO₂ nanoparticles (darker spots) are all present in the polymer particles in both cases (**Figure 1a and b**), and no one is present in the continuous water phase. It can be seen that the CeO₂ nanoparticles aggregates are more centered in the polymer particles synthesized using the first strategy whereas they are more close to the border of the polymer particle in the hybrids synthesized using the second strategy. The difference comes from the feeding strategy used in each case. When the neat monomer preemulsion strategy is used, the monomer entering the reactor in the semicontinuous process covers de hybrid seed particles containing the CeO₂ nanoparticles. However, in the case of the miniemulsion feeding, a large fraction of the entering hybrid droplets nucleates, and hence not all the fed monomer is used to grow the seed particles and as a consequence CeO₂ nanoparticles aggregates are not fully encapsulated.

Nevertheless, the encapsulation of inorganic nanoparticles inside polymer particles cannot be proved just by TEM images, as sometimes the micrographs are not conclusive enough. Therefore, TEM Tomography studies were carried out to a representative area of the hybrid latexes prepared following the seeded semibatch (mini)emulsion strategy presented so far. The results demonstrated that the CeO₂ nanoparticles were surrounded by polymer in all directions in both, the seed and the final polymer particles, demonstrating beyond any doubt the encapsulated morphology [54].

Furthermore, it is remarkable that every polymer particle contains one CeO₂ nanoparticle aggregate in average. In **Figure 1a and b** it can be seen that the number of polymer particles with zero, two and three nanoparticles is very small. It is observed that the CeO₂ aggregate size increases with the nanoceria content in the formulation of the hybrid nanocomposite; namely, the higher the CeO₂ content, the larger the aggregates. **Figure 1c and d** presents the quantification of the CeO₂ aggregate sizes in the hybrid latexes containing 1 and 5% of CeO₂ nanoparticles. As it can be seen, aggregate sizes between 3 and 73 nm can be found for the hybrid latex containing 1% of CeO₂ nanoparticles, whereas aggregate sizes between 3 and 123 nm can be found for the nanocomposite containing 5% of CeO₂ nanoparticles. Volume average aggregate sizes are 26 and 50 nm, respectively. However, it should be mentioned that the initial average size of the CeO₂ nanoparticles dispersed in the monomer mixture was 12 nm (measured by

dynamic light scattering). Therefore, it seems that all the nanoparticles present in each monomer droplet aggregate during the first stages of the polymerization process to form a CeO₂ aggregate per polymer particle. This effect will be discussed deeply in the following section.

One of the main advantages of having inorganic nanoparticles encapsulated in polymer particles is the lack of agglomeration during the film formation process, obtaining homogeneous distribution of the nanoparticles in the polymeric film and avoiding their leaching during the lifetime of the coating. **Figure 1e** and **f** show the hybrid films obtained after drying hybrid latexes with 1 and 5% of CeO₂ nanoparticles. It can be seen that after film formation the nanoceria aggregates are homogeneously dispersed in the polymer matrix in both cases. The average CeO₂ aggregate size was also analyzed and it was found that the average size in volume of the CeO₂ nanoparticles in the film is 26 nm for the film containing 1% of CeO₂ and 46 nm for the film with 5% of CeO₂. Therefore, the average size of the CeO₂ aggregates does not change during the film formation process in which the polymer particles coalesce between them, indicating that the encapsulation is an efficient method to avoid the agglomeration of the inorganic nanoparticles in the final film.

3. Evolution of particle morphology during the synthesis of acrylic/CeO₂ hybrid nanocomposites synthesized by miniemulsion polymerization

The morphology obtained in a hybrid nanocomposite may affect directly the final application of the composite material as it has been shown in Section 1 of this chapter. The particle morphology will develop during the polymerization and the final particle morphology will be determined by the interplay of thermodynamics and kinetics. The equilibrium morphology is the one that minimizes the total interfacial energy (θ) of the system, for an organic/inorganic system being the organic phase polymer (monomer), and it is given by:

$$\theta = A_{PW} \cdot \gamma_{PW} + A_{IW} \cdot \gamma_{IW} + A_{IP} \cdot \gamma_{IP} + A_{II} \cdot \gamma_{II} \quad (1)$$

where, A_{ij} and γ_{ij} are the interfacial area and interfacial tensions respectively, between phase i and j , where P, I and W are polymer (monomer), inorganic material, and aqueous phase, respectively. In this particular case the CeO₂ inorganic nanoparticles were previously modified in order to make them hydrophobic and more compatible with the monomers, so the interfacial tension γ_{II} should be very low because when the inorganic particles come into contact, the contact occurs between the same hydrophobic materials. Neglecting γ_{II} , Eq. (1) reduces to an equation that has the same mathematical form that the equation used to calculate equilibrium morphologies of two phase polymer-polymer systems [58–60]. Using the morphology map developed in these studies, Asua showed a similar one (see **Figure 2**) adapted to a polymer/inorganic system [61], where the gray phase represents the inorganic material and the white the polymer (monomer).

According to this morphology map presented in **Figure 2**, the possible equilibrium morphologies that can be obtained in a polymer/inorganic hybrid nanocomposite are core-shell

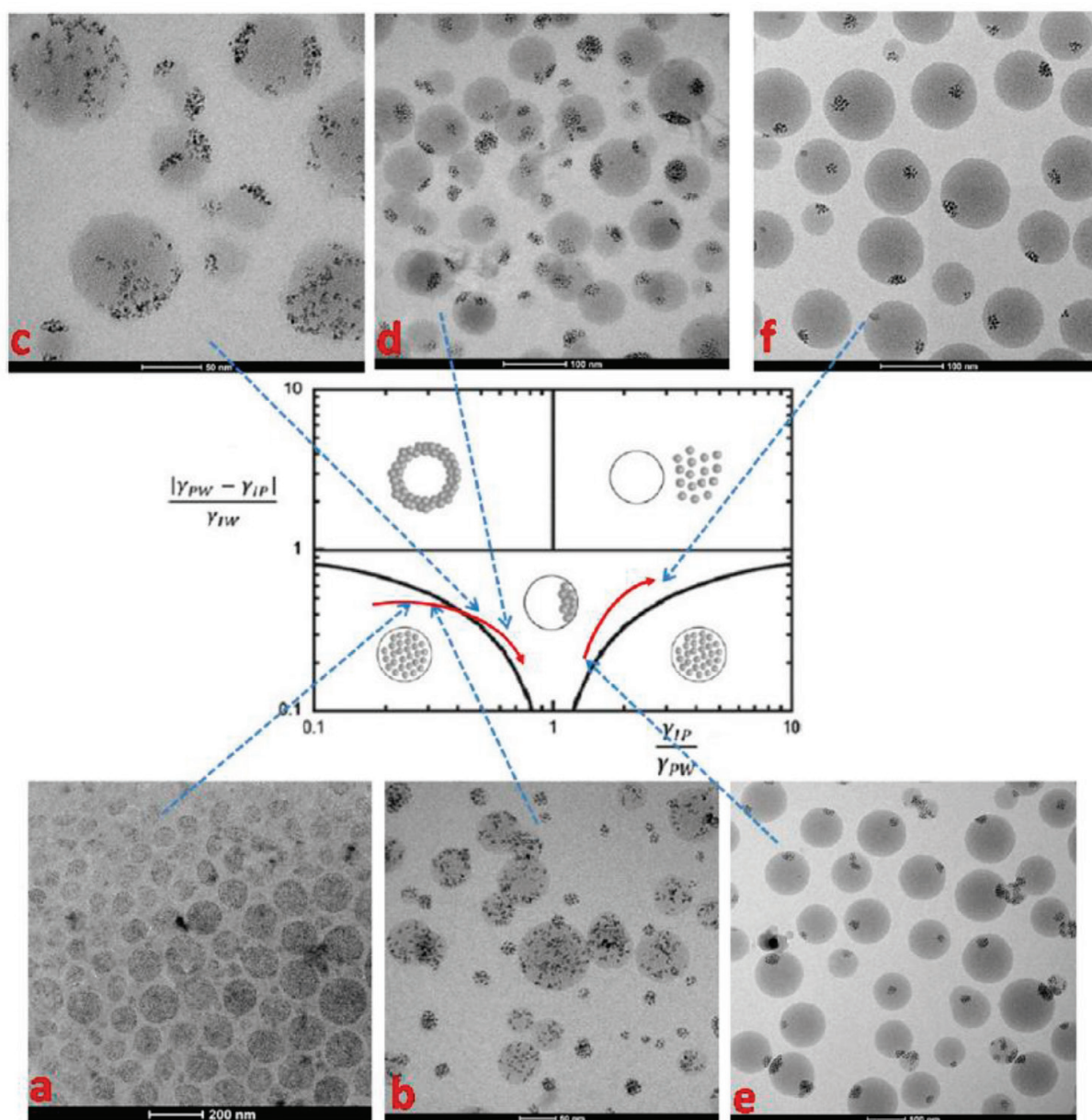


Figure 2. Morphology map and evolution of the particle morphology for (a) acrylic/CeO₂ monomer droplets, (b) 1% monomer conversion, (c) 8% monomer conversion, (d) 18% monomer conversion, (e) 40% monomer conversion, and (f) 100% conversion. Reprinted from [67] with permission from ACS Publications.

(encapsulated), inverted core-shell, hemispherical or separated particles. During the miniemulsion polymerization, the system and thus, the composition of the monomer droplets, are changing as polymerization proceeds. The monomer becomes polymer, initiator or other compounds may incorporate into the polymer and grafting might occur between the polymer being formed and the inorganic material. All these factors will alter the interfacial tensions between the phases and hence, the final equilibrium morphology. In this way, it would be possible to shift from encapsulated morphologies in the initial miniemulsion to hemispherical or separated phases after polymerization. There are some examples in the literature in which the initiator type [62, 63], emulsifier amount [64] and monomer type [65] variations affected strongly the final particle morphology.

In order to analyze the effect that polymerization may have on the morphology of the system described in this chapter, the evolution of the acrylic/CeO₂ nanocomposite is followed during the polymerization process (the hybrid seed preparation by batch miniemulsion polymerization) by cryo-TEM, analyzing samples withdrawn from the reactor at different monomer conversion, and the morphology map (**Figure 2**) is used as a reference to explain the different morphologies obtained, even if some of the morphologies presented are not at equilibrium. It can be observed that at the beginning in the miniemulsion, the CeO₂ nanoparticles are well dispersed in the monomer droplets (**Figure 2a**). This means that the compatibility of the nanoceria with the monomer mixture is really good in the monomer droplets or in other words, that the interfacial tension between the acrylic monomers and the inorganic material, γ_{IP} is low and the interfacial tension between the CeO₂ nanoparticles and water, γ_{IW} is high. This morphology is presented by the core-shell morphology on the left side where $\gamma_{IP}/\gamma_{PW} < 1$ and $|\gamma_{PW} - \gamma_{IP}|/\gamma_{IW} < 1$. It should be mentioned that the nanoparticles are sterically stabilized by the hydrophobic modification they bear in the monomer droplets.

In **Figure 2b** the acrylic/CeO₂ nanocomposite system at 1% of conversion is shown. The morphology observed is completely different, as the nanoparticles tend to aggregate, which means that the incompatibility between the newly formed polymer and the surface of the CeO₂ nanoparticles has increased or that γ_{IP} has become higher. This change in the morphology with the presence of polymer is observed too when the acrylic/CeO₂ hybrid miniemulsion is prepared adding a polymer in order to increase the stability of the miniemulsion [66]. At 8% of conversion, the difference becomes more evident, the nanoparticles are more aggregated and they tend to move towards the border of the polymer particles. The fraction of the polymer increases and thus, γ_{IP} increases. This way, the equilibrium morphology evolves following the red arrow crossing to the hemispherical region as shown in **Figure 2**. At 18 and 40% of conversion the CeO₂ aggregates are more compact and most of the aggregates are situated in the border of the polymer particle (equilibrium position). It should be mentioned that all these morphologies are not at equilibrium, since more than one nanoceria aggregate can be found in the polymer particles. However, when full conversion is achieved, one single aggregate can be seen in each polymer particle, which corresponds to the hemispherical equilibrium morphology.

In the literature there are some mathematical models to predict equilibrium morphologies of hybrid systems [51, 59, 61]. However, these models are not enough to explain the evolution of the acrylic/CeO₂ hybrid nanocomposites, since equilibrium morphology is not obtained until 40% of conversion is reached. Recently, Hamzelou et al. [67] developed a mathematical model for the dynamic evolution of this particular nanocomposite system. This approach provides the distribution of particle morphologies in the whole population of polymer particles. The distribution of particle morphologies is described by a distribution of clusters of CeO₂ nanoparticles (aggregates) dispersed in the monomer phase (see **Figure 3**). According to their position in the particles, the clusters are divided into two different categories: those at equilibrium positions (red dashed line in **Figure 3**) and clusters at non-equilibrium positions (blue line in **Figure 3**). Thermodynamics are used to calculate the equilibrium morphology and all relevant kinetic events of the system including cluster nucleation, polymerization, polymer diffusion and cluster aggregation are taken into account. **Figure 3** shows the simulated weight distributions for the CeO₂ aggregates (clusters). It is shown that at 1% of conversion, most of the nanoceria aggregates are in nonequilibrium positions. At 18% of conversion, most of

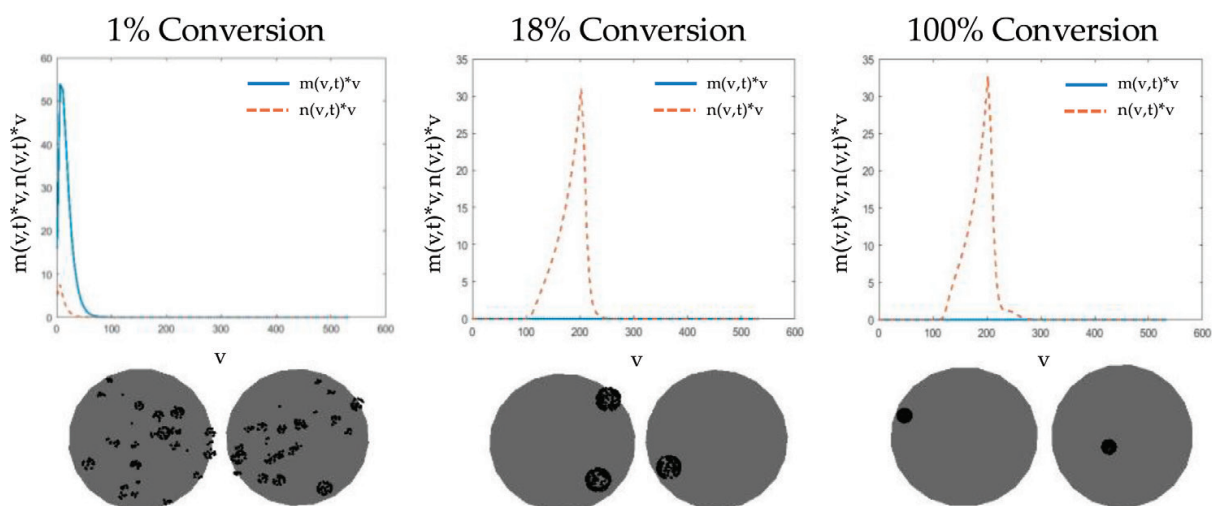


Figure 3. Simulated weight distributions (m and n represent aggregates in non-equilibrium and equilibrium positions, respectively) and the TEM-like images obtained from the distributions. Reprinted from [67] with permission from ACS Publications.

the aggregates are at equilibrium, however, in some of the polymer particles more than one aggregate can be found. At 100% conversion all the nanoceria aggregates are in equilibrium. TEM-like images are generated and they can be compared to the cryo-TEM images presented in **Figure 2**. It can be seen that CeO₂ nanoparticles aggregates follow the same evolution in the experimental cryo-TEM images and in the TEM-like images generated from the model.

To summarize, the morphology evolution of the whole acrylic/CeO₂ nanocomposite is as follows. During the first step, homogeneous distribution of the CeO₂ nanoparticles in the monomer droplets is obtained in the hybrid miniemulsion. During the miniemulsion polymerization, the CeO₂ nanoparticles aggregate and migrate to the surface of the polymer particles. Up to 40% of conversion, the concentration of monomer is high enough and the nanoparticles are able to move inside the monomer droplets towards equilibrium positions. Thus, the nanoceria aggregates are at the edge of the polymer particles, mostly surrounded by polymer, but not always encapsulated [66]. During the second step (neat monomer feeding), the migration of the CeO₂ aggregates is constrained due to the high internal viscosity of the particles. The monomer feeding is done under starved conditions and thus, the seed hybrid particles are covered by a shell of polymer leading to an encapsulated morphology. The proposed mechanism is graphically described in **Figure 4**.

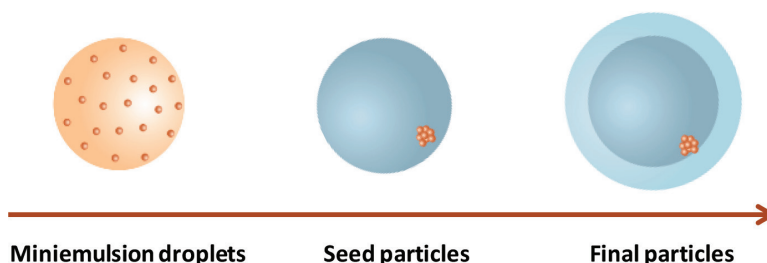


Figure 4. Schematic representation of the morphology evolution of the acrylic/CeO₂ nanocomposite system.

4. UV absorption properties of acrylic/CeO₂ hybrid nanocomposites

One of the main reasons to incorporate the CeO₂ nanoparticles into waterborne clear coatings is their excellent UV absorption capacity. This can be assessed by measuring the UV absorbance of 50 μm thick hybrid films. It should be mentioned that all the hybrid films are transparent and yellowish (**Figure 5**). The color of the films increases with the CeO₂ nanoparticle content from 1 to 5 wt% and hence, the transparency decreases. Even if the dispersion of the nanoparticles is good in all the hybrid films, the large sizes measured for the hybrid film containing 5% of CeO₂ nanoparticle affect the transparency.

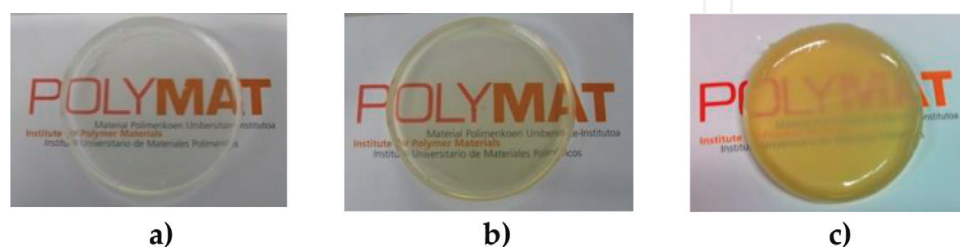


Figure 5. Picture of films cast at room temperature for different CeO₂ loadings: (a) 0% CeO₂, (b) 1% CeO₂ and (c) 5% CeO₂.

Figure 6 shows that the UV absorption of the hybrid films is higher in the presence of the nanocerium in the whole spectrum range (250–600 nm), but the absorption enhancement is most noticeable above 300 nm, where the pristine copolymer absorption is negligible. Furthermore, the higher the amount of CeO₂ nanoparticles, the higher the absorption. However, scattering is observed for the film containing 5% of CeO₂ nanoparticles due to the large size of aggregates obtained for this nanocomposite.

Photodegradation of the hybrid film is a major concern due to the photocatalytic activity of the CeO₂ nanoparticles. In the literature, the photodegradation of hybrid acrylic coatings has been studied in different substrates such as glass, stone or wood [68–71]. In these cases, the hybrid film was tested in a substrate and there might be two sources of radicals. One coming from the substrate and the other one from the nanoparticles present in the polymer matrix. To skip this problem the degradation behavior of the bare acrylic/CeO₂ hybrid films was analyzed. Accelerated weathering tests were conducted in a solar box, for the nanocomposite film without nanoparticles and for the one containing 1% of CeO₂. Different properties of the hybrid films exposed to UV light were measured [72]. Thermal properties reveal one step thermal degradation (around 380°C) and negligible changes in the glass transition temperature (T_g) values for all the hybrid films before and after the exposure. Regarding the microstructure, molecular weight distributions (MWD) and the formation of cross-linked or gel structures were also analyzed. The results show that there is degradation of the polymeric film since the cross-linked fraction increases in the films, but there is no additional effect in the films containing metal oxide nanoparticles. On the other hand, neither the Fourier Transform Infrared Spectra (FTIR) nor the TEM micrographs show any significant difference in the films. It is therefore concluded that the possible photodegradation that CeO₂ nanoparticles may produce in the bare hybrid films is negligible, owing to the similar properties obtained for the blank film and the hybrid film containing 1% CeO₂ nanoparticles after the UV irradiation.

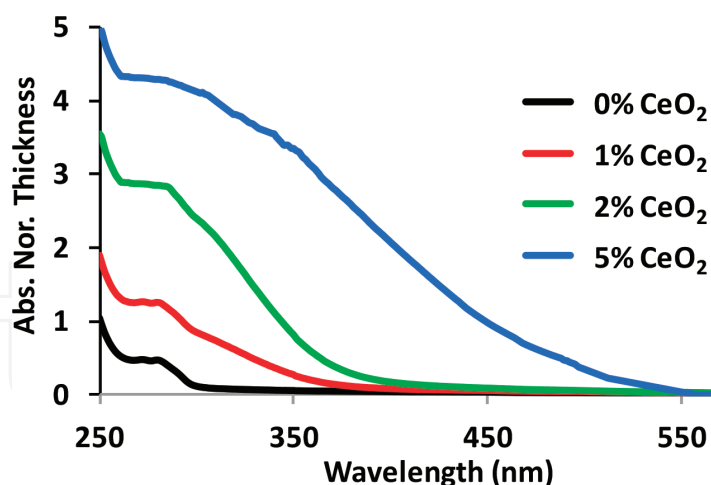


Figure 6. UV-vis absorption capacity of 50 μm hybrid films.

To study the effect of different metal oxides nanoparticles, a nanocomposite film with 1% ZnO nanoparticles was also synthesized following the same seeded semibatch polymerization approach as described in Section 2 [34]. The morphology obtained in the final hybrid films was different to that obtained for the CeO₂ hybrid films. The ZnO nanoparticles aggregate sizes were much bigger (~75 nm), preventing the homogeneous distribution of the nanoparticles in the film. However, the acrylic/ ZnO hybrid films presented higher UV absorption above 350 nm than the counterpart hybrids with CeO₂. In the photodegradation studies carried out in the work mentioned above [72], even if it is known that the photocatalytic activity of the ZnO is larger than that of the CeO₂, as it was mentioned in the introduction, the behavior of the hybrid films containing both types of nanoparticles did not differ significantly.

5. Conclusions and future perspectives

A polymerization strategy to synthesize waterborne hybrid acrylic/CeO₂ nanocomposites for their application as UV blocking coatings has been discussed in this Chapter. The designed two-step polymerization approach is able to produce different loadings of CeO₂ nanoparticles with industrially relevant solids content. Moreover, the strategy ensures the encapsulation of the nanoparticles in the polymer particles that avoids agglomeration during film formation process and provides good UV absorption properties, making these coatings good candidates as clear coats for outdoor applications. A mathematical model developed to predict the evolution of the particle morphology for polymer-polymer systems has been applied for the polymer-CeO₂ hybrids and it is able to predict the evolution of the morphology of the two stage semicontinuous polymerization opening the door to the use of the model for optimization and control of waterborne polymer-inorganic particle morphology purposes.

The designed strategy opens the possibility to encapsulate other nanoparticles and extend the application region. The incorporation of hydrophobically modified ZnO nanoparticles has also been tested, providing film forming hybrid latexes with improved UV absorption capacity [73]. Moreover, with the incorporation of a fluorinated monomer to the acrylic/ZnO hybrid system,

anticorrosion properties have been improved. It was demonstrated that the incorporation of the ZnO nanoparticles by blending was not enough to improve the corrosion protection, whereas when the nanoparticles were encapsulated and hence, well distributed in the polymeric film, the benefits were substantial [74]. Recently, many authors' investigation has been directed to improve anticorrosion properties with the incorporation of CeO₂ nanoparticles. For instance, polyurethane coatings containing CNT/CeO₂ [10], polyacrylic acid/CeO₂ coatings [11], CeO₂/graphene-epoxy nanocomposite coatings [12] and water based polyurethane/ CeO₂ coatings [13]. None of these works obtained encapsulated morphology and hence, the possible aggregation of the nanoparticles during film formation and leaching could be a problem, even though the anticorrosion properties were improved in all the cases. This means that combining the strategy developed in this work, with the appropriate monomers and the anticorrosion properties that CeO₂ nanoparticles exhibit in all the works mentioned above, synergetic effects could be obtained making these nanocomposites ideal candidates for corrosion protection.

Very recently, De San Luis et al. [75] incorporated quantum dots into core-shell particles made of polystyrene/divinyl benzene (DVB) as core and PMMA/DVB as shell. The cross-linked polymeric phases were synthesized in two stages following the strategy developed in this Chapter. Thanks to the encapsulated morphology obtained, the fluorescence emission of the QD containing core-shell particles was preserved for more time than any other work published so far. The same authors incorporated CeO₂ nanoparticles obtaining PS/QD/CeO₂/PMMA hybrid particles. Interestingly, the films casted from these hybrid particles exhibit increasing fluorescence under sunlight exposure [76]. This opens the possibility to use CeO₂ nanoparticles to enhance the optical properties of different technological devices.

Acknowledgements

Financial support from the Basque Government ELKARTEK KK-2016/00030 and KK-2017/00089 is greatly acknowledged. Miren Aguirre thanks the financial support given by the European Union (Woodlife project FP7-NMP-2009-SMALL-246434), the UPV/EHU (2984/2014) "Doktore berriak kontratatze eta horiek doktorego ondoko prestakuntza programetan sartzeko laguntza" and also the financial support received from Ministerio de Economía y Competitividad de España, Juan de la Cierva en Formación (FJCI-2014-22336). The SGIker UPV/EHU for the electron microscopy facilities of the Gipuzkoa unit is acknowledged. Programa de Grupos Consolidados from the Basque Government (IT999-16) is also gratefully acknowledged.

Author details

Miren Aguirre*, María Paulis and Jose R. Leiza

*Address all correspondence to: miren.aguirre@ehu.eus

POLYMAT and Kimika Aplikatua Saila, Kimika Zientzien Fakultatea, University of the Basque Country UPV/EHU, Donostia-San Sebastián, Spain

References

- [1] Yamaguchi I, Watanabe M, Shinagawa T, Chigane M, Inaba M, Tasaka A, et al. Preparation of core/shell and hollow nanostructures of cerium oxide by electrodeposition on a polystyrene sphere template. *ACS Applied Materials & Interfaces*. 2009;**1**(5):1070-1075
- [2] Fischer V, Lieberwirth I, Jakob G, Landfester K, Muñoz-Espí R. Metal oxide/polymer hybrid nanoparticles with versatile functionality prepared by controlled surface crystallization. *Advanced Functional Materials*. 2013;**23**:451-466
- [3] Mari M, Müller B, Landfester K, Muñoz-Espí R. Ceria/polymer hybrid nanoparticles as efficient catalysts for the hydration of nitriles to amides. *ACS*. 2015;**7**(20):10727-10733
- [4] Anjana PS, Deepu V, Uma S, Mohanan P, Philip J, Sebastian MT. Dielectric, thermal, and mechanical properties of CeO₂-filled HDPE composites for microwave substrate applications. *Journal of Polymer Science Part B: Polymer Physics*. 2010;**48**(9):998-1008
- [5] Chen Y, Mu W, Lu J. Young's modulus of PS/CeO₂ composite with core/shell structure microspheres measured using atomic force microscopy. *Journal of Nanoparticle Research*. 2012;**14**(2):696
- [6] Hu J, Zhou Y, He M, Yang X. Novel polysiloxane@CeO₂-PMMA hybrid materials for mechanical application. *Materials Letters*. 2014;**116**:150-153
- [7] Ansari AA, Khan MAM, Khan MN, Alrokayan SA, Alhoshan M, Alsalhi MS. Optical and electrical properties of electrochemically deposited polyaniline/CeO₂ hybrid nanocomposite film. *Journal of Semiconductors*. 2011;**32**(4):043001-1-043001-6
- [8] Incel A, Güner T, Parlak O, Demir MM. Null extinction of ceria@silica hybrid particles: Transparent polystyrene composites. *Applied Materials & Interfaces*. 2015;**7**:27539-27546
- [9] Hu J, Zhou Y. The properties of nano (ZnO-CeO₂) polysiloxane core-shell microspheres and their application for fabricating optical diffusers. *Applied Surface Science*. 2016;**365**:166-170
- [10] Kumar AM, Rahman MM, Gasem ZM. A promising nanocomposite from CNTs and nano-ceria: Nanostructured fillers in polyurethane coatings for surface protection. *RSC Advances*. 2015;**5**:63537-63544
- [11] Eduok U, Jossou E, Tihamiyu A, Omale J, Szpunar J. Ceria/acrylic polymer microgel composite: Synthesis, characterization, and anticorrosion application for API 5L X70 substrate in chloride-enriched medium. *Industrial and Engineering Chemistry Research*. 2017;**56**:5586-5597
- [12] Xia W, Zhao J, Wang T, Song L, Gong H, Guo H, et al. Anchoring ceria nanoparticles on graphene oxide and their radical scavenge properties under gamma irradiation environment. *Physical Chemistry Chemical Physics*. 2017;**19**:16785-16794
- [13] Ferrel-Álvarez AC, Domínguez-Crespo MA, Torres-Huerta AM, Cong H, Brachetti-Sibaja SB, López-Oyama AB. Intensification of electrochemical performance of AA7075 aluminum alloys using rare earth. *Polymers (Basel)*. 2017;**9**(178):1-23

- [14] Khan SB, Faisal M, Rahman MM, Jamal A. Exploration of CeO₂ nanoparticles as a chemi-sensor and photo-catalyst for environmental applications. *Science of the Total Environment*. 2011;**409**(15):2987-2992
- [15] Faisal M, Khan SB, Rahman MM, Jamal A, Akhtar K, Abdullah MM. Role of ZnO-CeO₂ nanostructures as a photo-catalyst and chemi-sensor. *Journal of Materials Science and Technology*. 2011;**27**(7):594-600
- [16] Arshad T, Khan SA, Faisal M, Shah Z, Akhtar K, Asiri AM, et al. Cerium based photo-catalysts for the degradation of acridine orange in visible light. *Journal of Molecular Liquids*. 2017;**241**:20-26
- [17] Khan SB, Karimov KS, Chani MTS, Asiri AM, Akhtar K, Fatima N. Impedimetric sensing of humidity and temperature using CeO₂-Co₃/O₄ nanoparticles in polymer hosts. *Microchimica Acta*. 2015;**182**(11-12):2019-2026
- [18] Marwani HM, Bakhsh EM, Khan SB, Danish EY, Asiri AM. Cerium oxide-cadmium oxide nanomaterial as efficient extractant for yttrium ions. *Journal of Molecular Liquids*. 2018;**269**:252-259
- [19] Katangur P, Patra PK, Warner SB. Nanostructured ultraviolet resistant polymer coatings. *Polymer Degradation and Stability*. 2006;**91**:2437-2442
- [20] Jaroenworoluck A, Sunsaneeyametha W, Kosachan N, Stevens R. Characteristics of silica coated TiO₂ and its UV absorption for sunscreen cosmetic applications. *Surface and Interface Analysis*. 2006;**38**:473-477
- [21] Nagasawa H, Xu J, Kanezashi M, Tsuru T. Atmospheric-pressure plasma-enhanced chemical vapor deposition of UV-shielding TiO₂ coatings on transparent plastics. *Materials Letters*. 2018;**228**:479-481
- [22] Weichelt F, Emmler R, Flyunt R, Beyer E, Buchmeiser MR, Beyer M. ZnO-based UV nanocomposites for wood coatings in outdoor applications. *Macromolecular Materials and Engineering*. Nov. 2010;**295**:130-136
- [23] Zhao H, Li RKY. A study on the photo-degradation of zinc oxide (ZnO) filled polypropylene nanocomposites. *Polymer (Guildf)*. Apr. 2006;**47**(9):3207-3217
- [24] Masui T, Yamamoto M, Sakata T, Mori H, Adachi GY. Synthesis of BN-coated CeO₂ one powder as a new UV blocking material. *The Royal Society of Chemistry*. 2000;**10**:353-357
- [25] Aguirre M, Paulis M, Leiza JR. UV screening clear coats based on encapsulated CeO₂ hybrid latexes. *Journal of Materials Chemistry A*. 2013;**1**(9):287-292
- [26] Althues H, Henle J, Kaskel S. Functional inorganic nanofillers for transparent polymers. *Chemical Society Reviews*. Sep. 2007;**36**(9):1454-1465
- [27] Chiu F-C, Lai C-M. Optical and electrical characterizations of cerium oxide thin films. *Journal of Physics D: Applied Physics*. 2010;**43**(7):075104
- [28] Christensen PA, Dilks A, Egerton TA. Infrared spectroscopic evaluation of the photodegradation of paint. Part I. The UV degradation of acrylic films pigmented with titanium dioxide. *Journal of Materials Science*. 1999;**34**:5689-5700

- [29] Du J, Sun H. Polymer/TiO₂ hybrid vesicles for excellent UV screening and effective encapsulation of antioxidant agents. *ACS Applied Materials & Interfaces*. 2014;**6**(16):13535-13541
- [30] Hu J, Gao Q, Xu L, Zhang M, Xing Z, Guo X, et al. Significant improvement in thermal and UV resistances of UHMWPE fabric through in situ formation of polysiloxane-TiO₂ hybrid layers. *ACS Applied Materials & Interfaces*. 2016;**8**(35):23311-23320
- [31] Hu J, Gao Q, Xu L, Wang M, Zhang M, Zhang K, et al. Functionalization of cotton fabrics with highly durable polysiloxane-TiO₂ hybrid layers: Potential applications for photo-induced water-oil separation, UV shielding, and self-cleaning. *Journal of Materials Chemistry A*. 2018;**6**(14):6085-6095
- [32] Li YQ, Fu SY, Mai YW. Preparation and characterization of transparent ZnO/epoxy nanocomposites with high-UV shielding efficiency. *Polymer*. Mar. 2006;**47**(6):2127-2132
- [33] Lu H, Fei B, Xin JH, Wang R, Li L. Fabrication of UV-blocking nanohybrid coating via miniemulsion polymerization. *Journal of Colloid and Interface Science*. Aug. 2006;**300**(1):111-116
- [34] Aguirre M, Barrado M, Iturrondobeitia M, Okariz A, Guraya T, Paulis M, et al. Film forming hybrid acrylic/ZnO latexes with excellent UV absorption capacity. *Chemical Engineering Journal*. 2015;**270**:300-308
- [35] Wang H, Qiu X, Liu W, Fu F, Yang D. A novel lignin/ZnO hybrid nanocomposite with excellent UV absorption ability and its application in transparent polyurethane coating. *Industrial and Engineering Chemistry Research*. 2017;**56**(39):11133-11141
- [36] Bennett SW, Keller AA. Comparative photoactivity of CeO₂, γ-Fe₂O₃, TiO₂ and ZnO in various aqueous systems. *Applied Catalysis B: Environmental*. Feb. 2011;**102**(3-4):600-607
- [37] Bourgeat-Lami E, Lansalot M. Organic/inorganic composite latexes: The marriage of emulsion polymerization and inorganic chemistry. *Advances in Polymer Science*. 2010;**233**:53-123
- [38] Zgheib N, Putaux JL, Thill A, D'Agosto F, Lansalot M, Bourgeat-Lami E. Stabilization of miniemulsion droplets by cerium oxide nanoparticles: A step toward the elaboration of armored composite latexes. *Langmuir*. 2012;**28**(14):6163-6174
- [39] González-Matheus K, Leal GP, Tollan C, Asua JM. High solids pickering miniemulsion polymerization. *Polymer*. 2013;**54**:6314-6320
- [40] González E, Bonnefond A, Barrado M, Casado Barrasa AM, Asua JM, Leiza JR. Photoactive self-cleaning polymer coatings by TiO₂ nanoparticle pickering miniemulsion polymerization. *Chemical Engineering Journal*. 2015;**281**:209-217
- [41] Bonnefond A, Ibarra M, Gonzalez E, Barrado M, Asua JM, Leiza JR, et al. Photocatalytic and magnetic titanium dioxide/polystyrene/magnetite composite hybrid polymer particles. *Polymer Chemistry*. 2016;**54**:3350-3356
- [42] Hawkett BS, Such CH, Nguyen DN, Farrugia JM, MacKinno OM. Surface polymerization process using RAFT agent for manufacture of polymer-encapsulated particulates. WO2006037161; 2006

- [43] Hawkett BS, Such CH, Nguyen DN. Polymer-encapsulated particulate material and interfacial polymerization process using RAFT agent. WO2007112503; 2007
- [44] Garnier J, Warnant J, Lacroix-Desmazes P, Dufils PE, Vinas J, Vanderveken Y, et al. An emulsifier-free RAFT-mediated process for the efficient synthesis of cerium oxide/polymer hybrid latexes. *Macromolecular Rapid Communications*. 2012;**33**(16):1388-1392
- [45] Garnier J, Warnant J, Lacroix-Desmazes P, Dufils PE, Vinas J, Van Herk A. Sulfonated macro-RAFT agents for the surfactant-free synthesis of cerium oxide-based hybrid latexes. *Journal of Colloid and Interface Science*. 2013;**407**:273-281
- [46] Warnant J, Garnier J, van Herk A, Dufils PE, Vinas J, Lacroix-Desmazes P. A CeO₂/PVDC hybrid latex mediated by a phosphonated macro-RAFT agent. *Polymer Chemistry*. 2013;**4**(23):5656-5663
- [47] Zgheib N, Putaux JL, Thill A, Bourgeat-Lami E, D'Agosto F, Lansalot M. Cerium oxide encapsulation by emulsion polymerization using hydrophilic macroRAFT agents. *Polymer Chemistry*. 2013;**4**(3):607
- [48] Weiss CK, Landfester K. Miniemulsion polymerization as a means to encapsulate organic and inorganic materials. *Hybrid Latex Part*. 2010;**233**:185-236
- [49] Asua JM. Challenges for industrialization of miniemulsion polymerization. *Progress in Polymer Science*. 2014;**39**(10):1797-1826
- [50] Paulis M, Asua JM. Knowledge-based production of waterborne hybrid polymer materials. *Macromolecular Reaction Engineering*. 2016;**10**:8-21
- [51] Reyes Y, Paulis M, Leiza JR. Modeling the equilibrium morphology of nanodroplets in the presence of nanofillers. *Journal of Colloid and Interface Science*. 2010;**352**(2):359-365
- [52] Asua JM. Miniemulsion polymerization. *Progress in Polymer Science*. 2002;**27**(7):1283-1346
- [53] Aguirre M, Paulis M, Leiza JR. UV screening clear coats based on encapsulated CeO₂ hybrid latexes. *Journal of Materials Chemistry A*. 2013;**1**:3155
- [54] Aguirre M, Paulis M, Leiza JR, Guraya T, Iturrondobeitia M, Okariz A, et al. High-solids-content hybrid acrylic/CeO₂ latexes with encapsulated morphology assessed by 3D-TEM. *Macromolecular Chemistry and Physics*. 2013;**214**:2157-2164
- [55] Aguirre M, Paulis M, Leiza JR. Particle nucleation and growth in seeded semi-batch miniemulsion polymerization of hybrid CeO₂/acrylic latexes. *Polymer*. 2014;**55**(3):752-761
- [56] Rodríguez R, Barandiaran MJ, Asua JM. Particle nucleation in high solids miniemulsion polymerization. *Macromolecules*. 2007;**40**:5735-5742
- [57] Aguirre M, Barrado M, Paulis M, Leiza JR. (Cryo)-TEM assessment of droplet nucleation efficiency in hybrid acrylic/CeO₂ semibatch miniemulsion polymerization. *Macromolecules*. 2014;**47**(23):8408-8410
- [58] González-Ortiz LJ, Asua JM. Development of particle morphology in emulsion polymerization. I. Cluster dynamics. *Macromolecules*. 1995;**28**:3135-3145

- [59] González-Ortiz LJ, Asua JM. Development of particle morphology in emulsion polymerization. II. Cluster dynamics in reacting systems. *Macromolecules*. 1996;**29**:383-389
- [60] González-Ortiz LJ, Asua JM. Development of particle morphology in emulsion polymerization. III. Cluster nucleation and dynamics in polymerizing systems. *Macromolecules*. 1996;**29**:4520-4527
- [61] Asua JM. Mapping the morphology of polymer-inorganic nanocomposites synthesized by miniemulsion polymerization. *Macromolecular Chemistry and Physics*. 2014;**215**(5): 458-464
- [62] Mori Y, Kawaguchi H. Impact of initiators in preparing magnetic polymer particles by miniemulsion polymerization. *Colloids and Surfaces. B, Biointerfaces*. 2007;**56**(1-2):246-254
- [63] Staudt T, Machado TO, Vogel N, Weiss CK, Araujo PHH, Sayer C, et al. Magnetic polymer/nickel hybrid nanoparticles via miniemulsion polymerization. *Macromolecular Chemistry and Physics*. 2013;**214**:2213-2222
- [64] Gong T, Yang D, Hu J, Yang W, Wang C, Lu JQ. Preparation of monodispersed hybrid nanospheres with high magnetite content from uniform Fe₃O₄ clusters. *Colloids and Surfaces A: Physicochemical and Engineering Aspects*. 2009;**339**:232-239
- [65] Qiao X, Chen MIN, Zhou J, Wu L. Synthesis of raspberry-like silica/polystyrene/silica multilayer hybrid particles via miniemulsion polymerization. *Journal of Polymer Science, Part A: Polymer Chemistry*. 2006;**45**:1028-1037
- [66] Aguirre M, Paulis M, Barrado M, Iturrondobeitia M, Okariz A, Guraya T, et al. Evolution of particle morphology during the synthesis of hybrid acrylic/CeO₂ nanocomposites by miniemulsion polymerization. *Journal of Polymer Science, Part A: Polymer Chemistry*. 2014;**53**:792-799
- [67] Hamzehlou S, Aguirre M, Leiza JR. Dynamics of the particle morphology during the synthesis of waterborne polymer-inorganic hybrids. *Macromolecules*. 2017;**50**:7190-7201
- [68] Lazzari M, Scaronone D, Malucelli G, Chiantore O. Durability of acrylic films from commercial aqueous dispersion: Glass transition temperature and tensile behavior as indexes of photooxidative degradation. *Progress in Organic Coatings*. 2011;**70**(2-3):116-121
- [69] Saha S, Kocaefe D, Krause C, Larouche T. Effect of titania and zinc oxide particles on acrylic polyurethane coating performance. *Progress in Organic Coatings*. 2011;**70**:170-177
- [70] Saha S, Kocaefe D, Boluk Y, Pichette A. Surface degradation of CeO₂ stabilized acrylic polyurethane coated thermally treated jack pine during accelerated weathering. *Applied Surface Science*. 2013;**276**:86-94
- [71] Serra CL, Tulliani JM, Sangermano M. An acrylic latex filled with zinc oxide by miniemulsion polymerization as a protective coating for stones. *Macromolecular Materials and Engineering*. 2014;**299**:1352-1361
- [72] Aguirre M, Goikoetxea M, Alberto L, Paulis M, Leiza JR. Accelerated ageing of hybrid acrylic waterborne coatings containing metal oxide nanoparticles: Effect on the microstructure. *Surface and Coating Technology*. 2017;**321**:484-490

- [73] Aguirre M, Barrado M, Iturrondobeitia M, Okariz A, Guraya T, Paulis M, et al. Film forming hybrid acrylic/ZnO latexes with excellent UV absorption capacity. *Chemical Engineering Journal*. 2015;**270**:300-308
- [74] Chimenti S, Vega JM, Aguirre M, Garcia-Lecina E, Diez JA, Grande H-J, et al. Effective incorporation of ZnO nanoparticles by miniemulsion polymerization in waterborne binders for steel corrosion protection. *Journal of Coatings Technology and Research*. 2017;**14**(4):829-839
- [75] De San Luis A, Bonnefond A, Barrado M, Guraya T, Iturrondobeitia M, Okariz A, et al. Toward the minimization of fluorescence loss in hybrid cross-linked core-shell PS/QD/PMMA nanoparticles: Effect of the shell thickness. *Chemical Engineering Journal*. 2017;**313**:261-269
- [76] Luis ADS, Paulis M, Leiza JR. Co-encapsulation of CdSe/ZnS and CeO₂ nanoparticles in waterborne polymer dispersions: Enhancement of fluorescence emission under sunlight. *Soft Matter*. 2017;**13**(44):8039-8047